Astronomy & Astrophysics

Dielectronic recombination data for dynamic finite-density plasmas

VII. The neon isoelectronic sequence

O. Zatsarinny[1],[*], T. W. Gorczyca[1], K. Korista[1], N. R. Badnell[2], and D. W. Savin[3]

[1] Department of Physics, Western Michigan University, Kalamazoo, Michigan, 49008-5252, US
  e-mail: oleg_zoi@yahoo.com; [gorczyca;korista]@wmich.edu
[2] Department of Physics, University of Strathclyde, Glasgow, G4 0NG, UK
[3] Columbia Astrophysics Laboratory, Columbia University, New York, 10027, USA
  e-mail: savin@astro.columbia.edu

Abstract. Dielectronic recombination (DR) and radiative recombination (RR) data for neon-like ions forming sodium-like systems has been calculated as part of the assembly of a DR database necessary for modelling of dynamic and/or finite-density plasmas (Badnell et al. 2003). Dielectronic recombination coefficients for neon-like ions from Na^+ to Zn^{20+}, as well as Kr^{26+}, Mo^{32+}, Cd^{38+}, and Xe^{44+}, are presented and the results discussed.

Key words. atomic data – atomic processes – plasmas

1. Introduction

Dielectronic recombination (DR) is an important recombination process for laboratory and astrophysical plasmas. Accurate DR rate coefficients are essential in the determination of the ionization balance and in the interpretation of most types of astrophysical spectra. The DR process has been subject to intense theoretical study, but the existing sophisticated calculations have been carried out only for specific ions, and most available data are based on simplified models. Recent experimental measurements (Savin et al. 1999, 2002) have demonstrated that many of the earlier computations of DR rate coefficients are inaccurate and that systematic computations with improved approximations are needed. A review of the published theoretical DR data for L-shell ions as of late 2001 is given by Savin & Laming (2002).

We have initiated a program to generate a total and final state level-resolved intermediate coupling DR database necessary for spectroscopic modelling of dynamic and/or finite density plasmas (Badnell et al. 2003). To this end, work has been underway in the calculation of DR data for the hydrogen through fluorine-like isoelectronic sequences and beyond. In this paper, we describe calculations and results for dielectronic recombination data for neon-like ions forming sodium-like systems.

Although studies for a few elements of this sequence have been made, there are no systematically determined DR rate coefficients for the entire sequence. The first calculations of DR rate coefficients for neon-like ions were carried out by Jacobs et al. (1977, 1979) for Mg, Si, S, and Fe atoms using a simplified model. In this model, the autoionization rates were obtained from the threshold values of the partial-wave electron-impact excitation cross sections for the corresponding ions by means of the quantum-defect theory relationship between these values. The excitation cross sections were obtained in the distorted-wave approximation in LS coupling, and only dipole 2s–3p, 2p–3s, and 2p–3d transitions were included. In addition, radiative decay of autoionizing states was approximated as the ionic core radiative decay rate. As we will discuss, this simplified model gives fairly accurate high-temperature DR rate coefficients for low-charged Mg^{2+}, but underestimates DR rate coefficients for the heavier Si^{4+}, S^{6+}, and Fe^{16+} ions by large factors at the peak in the DR rate coefficient.

The first sophisticated study of DR rate coefficients for neon-like ions was carried out by Chen (1986). The calculations were for seven ions with atomic number $18 \leq Z \leq 54$, and used the multiconfiguration Dirac-Fock (MCDF) model to evaluate detailed transition energies and rates. DR rate coefficients for 10 temperatures in the range $0.2 \leq T \leq 6$ keV were computed. Chen (1986) also studied the dependence of DR rate coefficients from the intermediate states $2p^5 3lnl'$ and $2p^5 4l4l'$ as functions of the principal quantum number n and orbital angular momentum l. One conclusion of his work was that

---
[*] *Present Address*: Physics Department, Drake University, Des Moines, IA 50311, US.

relativistic effects on total DR rate coefficients of neon-like ions are negligible; however, the LSJ splitting can give rise to a noticeable redistribution in partial DR rate coefficients. Calculations of DR rate coefficients for neon-like ions were also performed by Romanik (1988) in an LS coupling approximation for ions with low atomic number. The calculations of Romanik (1988) lie $\approx 15\%$ above those of Chen (1986) for Si^{4+} and agree very well for Fe^{16+}. The close agreement between the results of Chen and Romanik and the large difference between their data and results of Jacobs et al. (1977, 1979) strongly suggest inaccuracies in the reported results of Jacobs et al. (1977, 1979). The available DR data in the published literature were fitted by Mazzotta et al. (1998) for all neon-like ions from Na^+ to Ni^{18+}. They relied mainly on the results of Chen (1986) for ions heavier than argon and those of Romanik (1988) for lighter ions. For Na^+, Mazzotta et al. write that they used the calculations of Shull & Van Steenberg (1982), and for P^{5+} and Cl^{7+} that they adopted the data of Landini & Monsignori Fossi (1991) multiplied by a factor 4 to take into account the results of Romanik (1988) and Chen (1986) for adjacent ions.

More recently, Fournier et al. (1997) has reported results for neon-like Ar^{8+} and Gu (2003b) for neon-like Mg^{2+}, Si^{4+}, S^{6+}, Ar^{8+}, Ca^{10+}, Fe^{16+} and Ni^{18+} (see also Gu 2003a for Fe^{16+}). We discuss some of these results in Sect. 3. It is important for us to compare with these modern theoretical results and to confirm that various theoretical methods have converged to the same results, as there are no experimental measurements available for this isoelectronic sequence.
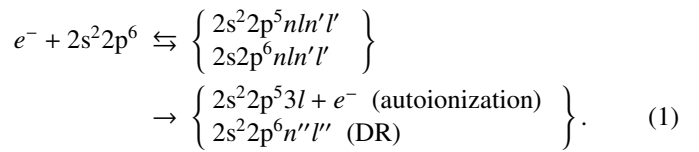
In this paper, we apply an intermediate-coupling multi-configuration Breit-Pauli (MCBP) method, in the isolated resonance approximation, to compute DR rate coefficients for neon-like ions from Na^+ to Zn^{20+}, as well as for Kr^{26+}, Mo^{32+}, Cd^{38+}, and Xe^{44+}. The rate coefficients computed here cover a wide range of temperatures and ionic species. The present calculations also attempt to produce final state-resolved DR rate coefficients which are important in modelling plasmas under certain conditions. Total DR rate coefficients, along with radiative recombination (RR) rate coefficients, are presented in compact form using simple fitting formulae. It is impractical to list all level-resolved rate coefficients in a paper publication. As previously discussed (Badnell et al. 2003), this latter data will form part of an Atomic Data and Analysis Structure (ADAS) dataset comprising the adf09 files for each ion, detailing the rate coefficients to each LSJ-resolved final state. This data is available through the ADAS project (Summers 1999) and is also made available online at the Oak Ridge Controlled Fusion Atomic Data Center http://www-cfadc.phy.ornl.gov/data_and_codes. In Sect. 2 we give a brief description of the theory used and the details of our calculations for the neon-like ions. In Sect. 3 we present the results for dielectronic recombination rate coefficients for the aforementioned ions in this sequence. We conclude with a brief summary in Sect. 4.

2. Theory

The theoretical details of our calculations have already been described in detail (Badnell et al. 2003; Zatsarinny et al. 2003).

Here we outline only the points specific to the present case. The calculation of the energy dependent DR cross sections were carried out using the code AUTOSTRUCTURE (Badnell 1986; Badnell & Pindzola 1989), which is based on lowest order perturbation theory where both the electron-electron and electron-photon interactions are treated to first order. This independent-processes, isolated-resonance approximation is used to compute configuration-mixed LS and IC energy levels, and radiative and autoionization rates, which are then used to compute Lorentzian DR resonance profiles. This enables the generation of final state level-resolved and total DR rate coefficients. We neglected interference between RR and DR, which we have shown does not affect the dominant rate coefficients (Zatsarinny et al. 2003).

The DR process for neon-like ions can be represented by

$$e^- + 2s^2 2p^6 \leftrightarrows \left\{ \begin{array}{l} 2s^2 2p^5 nln'l' \\ 2s 2p^6 nln'l' \end{array} \right\}$$
$$\rightarrow \left\{ \begin{array}{l} 2s^2 2p^5 3l + e^- \text{ (autoionization)} \\ 2s^2 2p^6 n''l'' \text{ (DR)} \end{array} \right\}. \quad (1)$$

Using the previous work on DR via $\Delta n = 1$ core electron excitations for L-shell ions by Chen (1986) and Zatsarinny et al. (2003) as a guide, we considered in our calculations only the $2 \rightarrow 3$ processes ($nl = 3l$), with $0 \le l' \le 6$ and $3 \le n' \le 1000$. We expect DR via $2 \rightarrow 4$ core excitation will contribute $\lesssim 4\%$ to the total DR rate coefficient. A bound orbital basis (1s, 2s, 2p, 3s, 3p, 3d) was generated from a Hartree-Fock (HF; Froese Fischer 1991) calculation for the $1s^2 2s^2 2p^5$ configuration to get the first three orbitals, followed by a configuration-average, frozen-core HF calculation for the $1s^2 2s^2 2p^5 3l$ states to get the additional $n = 3$ orbitals. Then the corresponding atomic structures for both initial-ion states and resonance and bound states of the recombining ion were obtained by diagonalizing the appropriate Breit-Pauli Hamiltonian. All target states were obtained with full configuration and spin-orbit mixing of the configurations indicated in Eq. (1). Distorted wave calculations were then performed to generate the appropriate free εl and bound $n'l'$ ($n' > 3$) orbitals, which are attached to each target state to yield the continuum and resonance states, respectively. All of the above orbitals are computed in the absence of any relativistic effects. However, the continuum and resonance states are subsequently re-coupled to an intermediate coupling scheme in order to include relativistic effects to lowest order. Also, the DR contribution from $3l3l'$ autoionizing states is considered separately, with full configuration and spin-orbital mixing between these states.

The computed DR cross section is a sum of Lorentzian profiles and can therefore be convoluted analytically with an experimental energy distribution, in order to compare to measured results, or with a Maxwellian electron distribution, in order to obtain total DR rate coefficients. This represents a huge savings in computational effort over R-matrix calculations since the latter must be performed for an extremely dense energy mesh in order to fully resolve all resonances (Gorczyca et al. 2002; Ramirez & Bautista 2002). The total DR rate coefficients were then fitted as

$$\alpha_{DR}(T) = T^{-3/2} \sum_i c_i e^{-E_i/T} \quad (2)$$

Table 1. Fitting coefficients for dielectronic and radiative recombination on neon-like ions forming sodium-like systems for Eqs. (2) and (3), respectively: c_1 and E_1 correspond to DR via the $3l3l'$ states in Eq. (1), c_2 and E_2 correspond to DR via the $3ln'l'(n' > 3)$ states in Eq. (1), and a, b, T_0, and T_1 correspond to RR. The coefficients c_i and a are in units of 10^{-11} cm^3 s^{-1}, the coefficients E_i, T_0, and T_1 are in eV, and b is dimensionless.

Ion	c_1	c_2	a	b	E_1	E_2	T_0	T_1
Na$^+$	2.359E+00	1.600E+01	1.381E+01	7.275E-01	2.626E+01	2.943E+01	7.230E-05	4.510E+00
Mg^{2+}	2.033E+01	9.120E+01	1.658E+01	6.707E-01	4.382E+01	5.224E+01	6.909E-04	1.870E+01
Al^{3+}	6.402E+01	3.548E+02	3.321E+01	6.986E-01	6.165E+01	7.854E+01	9.174E-04	4.874E+01
Si^{4+}	2.408E+02	1.023E+03	6.211E+01	7.336E-01	8.674E+01	1.104E+02	8.892E-04	8.769E+01
P^{5+}	5.058E+02	2.437E+03	9.735E+01	7.558E-01	1.061E+02	1.452E+02	9.266E-04	1.324E+02
S^{6+}	9.053E+02	4.652E+03	1.237E+02	7.632E-01	1.270E+02	1.820E+02	1.215E-03	1.959E+02
Cl^{7+}	1.567E+03	8.318E+03	1.584E+02	7.720E-01	1.487E+02	2.192E+02	1.397E-03	2.563E+02
Ar^{8+}	2.445E+03	1.293E+04	1.743E+02	7.716E-01	1.705E+02	2.601E+02	1.971E-03	3.406E+02
K^{9+}	3.536E+03	1.858E+04	1.966E+02	7.732E-01	1.927E+02	3.040E+02	2.490E-03	4.247E+02
Ca^{10+}	4.531E+03	2.704E+04	2.151E+02	7.738E-01	2.141E+02	3.508E+02	3.167E-03	5.145E+02
Sc^{11+}	6.193E+03	3.606E+04	2.367E+02	7.733E-01	2.384E+02	3.997E+02	3.858E-03	6.118E+02
Ti^{12+}	8.027E+03	4.588E+04	2.444E+02	7.698E-01	2.635E+02	4.512E+02	5.102E-03	7.513E+02
V^{13+}	9.445E+03	5.744E+04	2.612E+02	7.700E-01	2.899E+02	5.056E+02	6.133E-03	8.515E+02
Cr^{14+}	1.121E+04	6.982E+04	2.826E+02	7.700E-01	3.173E+02	5.621E+02	7.050E-03	9.913E+02
Mn^{15+}	1.354E+04	8.378E+04	2.889E+02	7.672E-01	3.446E+02	6.214E+02	8.838E-03	1.146E+03
Fe^{16+}	1.648E+04	9.888E+04	2.976E+02	7.649E-01	3.770E+02	6.878E+02	1.074E-02	1.316E+03
Co^{17+}	1.988E+04	1.123E+05	3.084E+02	7.633E-01	4.016E+02	7.464E+02	1.270E-02	1.487E+03
Ni^{18+}	2.388E+04	1.269E+05	3.201E+02	7.621E-01	4.314E+02	8.123E+02	1.477E-02	1.659E+03
Cu^{19+}	2.826E+04	1.417E+05	3.331E+02	7.611E-01	4.622E+02	8.803E+02	1.688E-02	1.834E+03
Zn^{20+}	3.307E+04	1.578E+05	3.477E+02	7.605E-01	4.937E+02	9.514E+02	1.899E-02	2.030E+03
Kr^{26+}	7.037E+04	2.437E+05	4.221E+02	7.561E-01	7.039E+02	1.425E+03	3.635E-02	3.327E+03
Mo^{32+}	1.121E+05	3.168E+05	4.720E+02	7.487E-01	9.462E+02	1.992E+03	6.583E-02	5.163E+03
Cd^{38+}	1.515E+05	3.796E+05	5.292E+02	7.440E-01	1.238E+03	2.658E+03	1.034E-01	7.368E+03
Xe^{44+}	1.923E+05	4.209E+05	6.112E+02	7.437E-01	1.576E+03	3.423E+03	1.391E-01	9.757E+03

to facilitate the further application of our data. Here the electron temperature T and the energy fitting parameter E_i are in units of eV, and the rate coefficient $\alpha_{DR}(T)$ is in units 10^{-11} cm^3 s^{-1}. Table 1 lists the fitting parameters c_i and E_i for each member of the neon-like sequence treated. The fits are accurate to within a maximum difference of 1% for 0.001 eV $< T <$ 100 000 eV. This covers the temperature range over which the ions investigated in this paper are predicted to form in both photoionization and collisional ionization equilibria. Note that the parameters c_i and E_i in Table 1 reflect different recombination channels in Eq. (1): c_1 and E_1 correspond to DR via the $3l3l'$ states whereas c_2 and E_2 correspond to DR via the $3ln'l'(n' > 3)$ states.

In order to provide total (DR + RR) recombination rate coefficients, Table 1 also contains the fitting coefficients for the RR rate coefficients. These were also obtained using the AUTOSTRUCTURE code with the same target orbitals and in the same approximation as the DR calculations. RR rate coefficients were fitted with the formula of Verner & Ferland (1996)

$$\alpha_{RR}(T) = a \left[\sqrt{T/T_0}\left(1 + \sqrt{T/T_0}\right)^{1-b} \left(1 + \sqrt{T/T_1}\right)^{1+b} \right]^{-1}, \quad (3)$$

where the fitting parameters T_0 and T_1 are in units of eV, a is in units of 10^{-11} cm^3 s^{-1}, and b is dimensionless. This form ensures the correct asymptotic behavior of the RR rate coefficients for low and high temperatures: $\alpha_{RR}(T) \propto T^{-1/2}$ at $T \ll T_0, T_1$, and $\alpha_{RR}(T) \propto T^{-3/2}$ at $T \gg T_0, T_1$. The average accuracy of the fitting is better than 4% in the temperature

range 10^{-5} eV to 10^{+5} eV (the error is less then 8% for all ions at all temperatures).

AUTOSTRUCTURE is implemented within the ADAS suite of programs as ADAS701. It produces raw autoionization and radiative rates which must be post-processed to obtain the final-state level-resolved and total DR rate coefficients. The post-processor ADASDR is used to reorganize the resultant data and also to add in radiative transitions between highly-excited Rydberg states, which are computed hydrogenically. This post-processor outputs directly the *adf09* file necessary for use by ADAS. The *adf09* files generated by our calculations in the IC configuration mixed approximations are available electronically (http://www-cfadc.phy.ornl.gov/data_and_codes). This site has tabulated DR rate coefficients into final LSJ levels from both the ground and metastable states in a manner useful to fusion and astrophysical modelers. Separate files *adf09* are produced for the $3l3l'$ states and the $3ln'l'(n' > 3)$ states, which are thus amenable to selective upgrade.
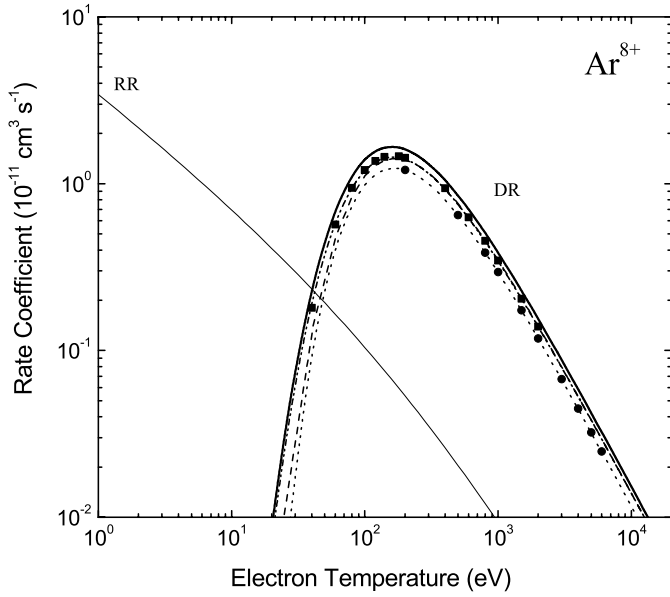
3. Results

Examples of the DR electron energy dependent resonance structure in the neon-like ions is given in Fig. 1 (there are no data from laboratory experiments to compare with). Here the DR cross sections have been convoluted with a cooler
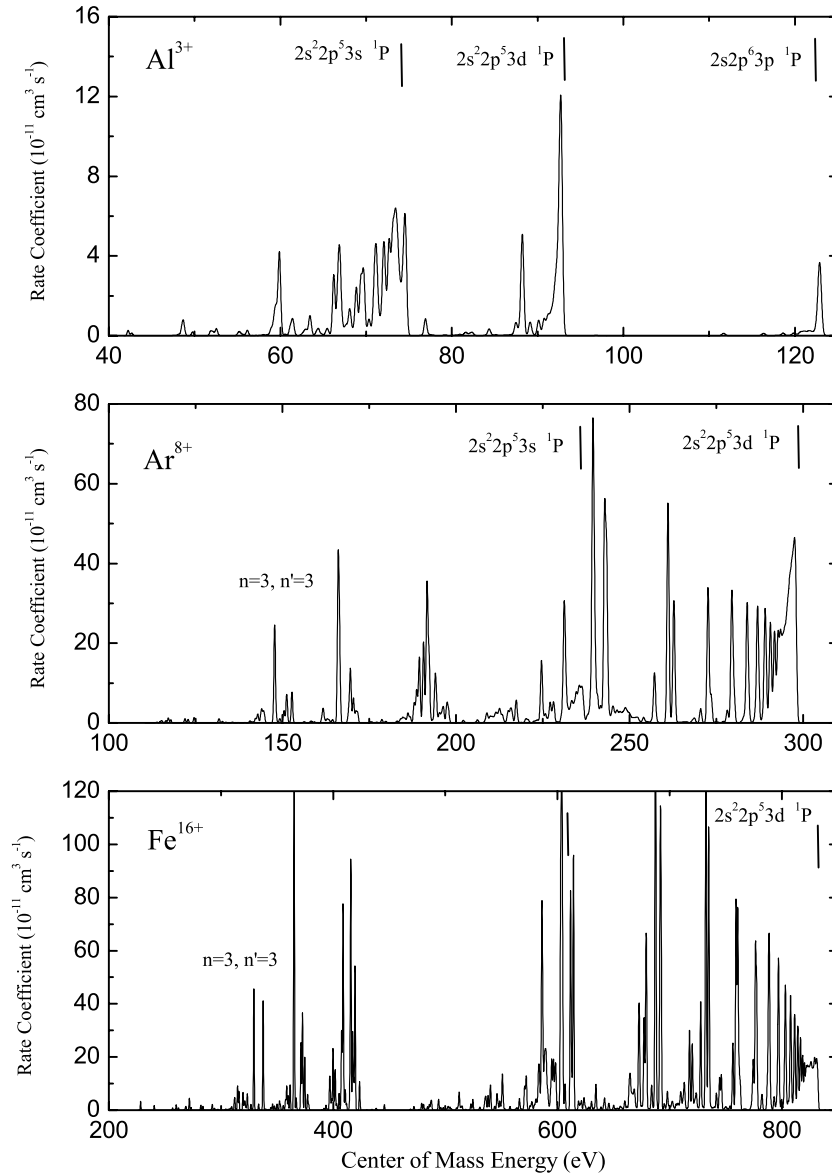
Fig. 1. DR resonance structure for neon-like ions Al^{3+}, Ar^{8+}, and Fe^{16+} forming sodium-like ions. The theoretical results have been convolved with a simulated experimental energy spread represented by a flattened Maxwellian with $k_B T_\perp = 15$ meV and $k_B T_\parallel = 0.15$ meV.

electron distribution which is characteristic of recent DR measurements using the heavy-ion Test Storage Ring (see, for example, Savin et al. 1999, 2002). The cooler electrons employed in this technique have an anisotropic Maxwellian distribution with low perpendicular and parallel temperatures of $k_B T_\perp \sim 15$ meV and $k_B T_\parallel \sim 0.15$ meV, which allows for detailed laboratory studies of the resonance structure. Figure 1 illustrates three examples of computed DR rate coefficients for low-, intermediate-, and high-charged neon-like ions. For low-charged Al^{3+}, all series with dipole-allowed core transitions ($e^- + 2s^2 2p^6 \rightarrow 2s2p^6 3pn'l'$, $2s^2 2p^5 3sn'l'$, $2s^2 2p^5 3dn'l'$) contribute appreciably, and the largest contributions come from the high-n' states. For intermediate-charged Ar^{8+}, the $2s^2 2p^5 3dn'l'$ series becomes relatively stronger, and the high-n' contributions are comparable to the lower-n' ones. For high-charged Fe^{16+}, the $2s^2 2p^5 3dn'l'$ series is now dominant, as are the low-n' resonances.

In Fig. 2, the Maxwellian DR rate coefficient for Ar^{8+} as a function of electron temperature is compared to other theoretical results. The MCDF results of Chen (1986), which were used in the critical compilation of Mazzotta (1998), are lower than ours by $\approx 25\%$; we attribute this difference to Chen's omission of certain intermediate states, such as $2s2p^6 3ln'l'$ and $2s^2 2p^5 3pn'l'$ ($n' > 3$). The results of Romanik (1988) are in somewhat better agreement with ours; the difference here we attribute to the approximate expressions for the autoionization and radiative rates used in that earlier work. Fournier et al. (1997) calculated DR for Ar^{8+} using the fully relativistic, parametric potential atomic structure code RELAC, with the continuum wave functions computed in the distorted-wave approximation. Gu (2003b) used a newly developed atomic package FAC, which uses relativistic multiconfigurational atomic wave functions. Both the results of Fournier et al. and Gu are in closer agreement with our results than are previously

Fig. 2. Maxwellian-averaged DR and RR rate coefficients for recombination of Ar^{8+} to Ar^{7+}. Present results for DR (*thick solid curve*) and RR (*thin solid curve*) were obtained in the MCBP calculations with the code AUTOSTRUCTURE. Also shown are the MCDF results of Chen (1986, *solid circles*), which were used for the compiled data of Mazzotta et al. (1998, *dotted curve*), the FAC results of Gu (2003b, *dash-dot-dotted curve*), the results of Romanik (1988, *dashed curve*), and the results of Fournier et al. (1997, *solid squares*) using the fully relativistic, parametric potential atomic structure code RELAC.
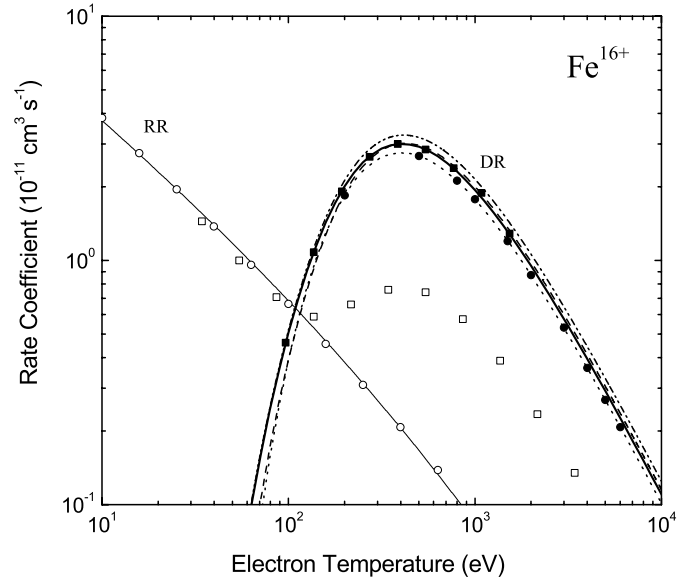

Fig. 3. Maxwellian-averaged DR and RR rate coefficients for recombination of Fe^{16+} to Fe^{15+}. Present results for DR (*thick solid curve*) and RR (*thin solid curve*) were obtained in the MCBP calculations with the code AUTOSTRUCTURE. Also shown are the MCDF results of Chen (1986, *solid circles*), which were used for the compiled data of Mazzotta et al. (1998, *dotted curve*), the FAC results of Gu (2003a, *solid squares*; 2003b, *dash-dot-dotted curve*), the results of Romanik (1988, *dashed curve*), the results of Jacobs et al. (1977, RR+DR, *open squares*), the RR results of Arnaud & Raymond (1992, *open circles*).

published calculations. The calculations of Fournier et al. and Gu both treat DR in the independent processes, isolated resonance approximation, as does Chen's MCDF code and AUTOSTRUCTURE. The agreement of our results with those from other recent independent calculations is an excellent consistency check on our applied methodology.

In Fig. 3, we make similar comparisons for Fe^{16+}. It is seen that the results of Chen (1986), as also used by Mazzotta (1998), Romanik (1988), and Gu (2003a,b) are all in fairly good agreement with our results. We expect the differences to be less than for Ar^{8+} because the inaccuracies introduced by either omitted configurations or approximate rate expressions decrease as the ionic charge increases, i.e., as the system becomes more hydrogenic. The results of Jacobs et al. (1977), however, are well below all the others ($\approx$factor of 4.0 near the peak rate coefficient). It is thus clear that the simplified methods used in the earlier calculations of Jacobs et al. (1977, 1979), which were discussed in Sect. 1, yielded inaccurate DR rate coefficients. Figure 3 shows that our computed RR rate coefficient as a function of temperature is in excellent agreement with that of Arnaud & Raymond (1992).

In Table 1, we present the fitting parameters for total DR and RR rate coefficients for each ion from Na^+ to Zn^{20+}, and also for Kr^{26+}, Mo^{32+}, Cd^{38+} and Xe^{44+}. In previous work, numerical calculations were performed for only certain ions in the sequence and the DR rate coefficients for all other ions were interpolated or extrapolated as a function of atomic number Z. This is not always a reliable approach, since, as we found in
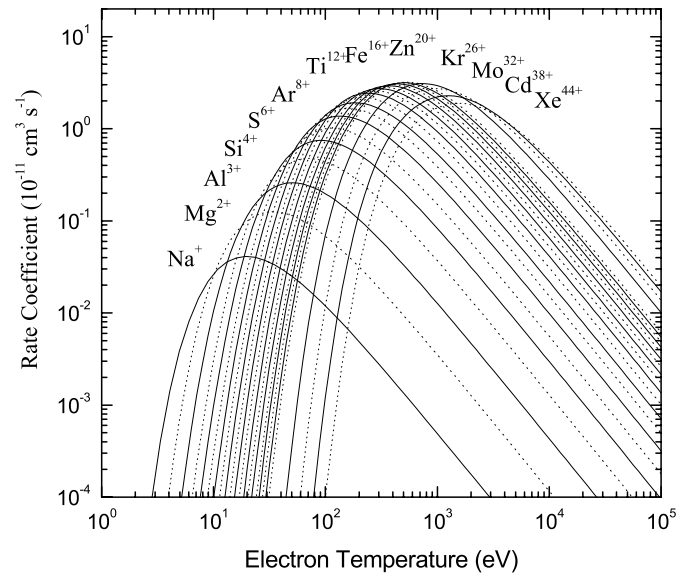
Fig. 4. Behavior of DR rate coefficients as a function of atomic number for the neon-like ions discussed in this paper forming sodium-like systems. Not all ions are labeled.

our study of oxygen-like ions (Zatsarinny et al. 2003), the rate coefficients for DR via $\Delta n = 0$ core excitations do not scale smoothly with Z. However, in the present case of neon-like ions, we have only $\Delta n = 1$ core excitations, which *do* scale smoothly with Z. Indeed, Fig. 4 clearly illustrates this behavior.
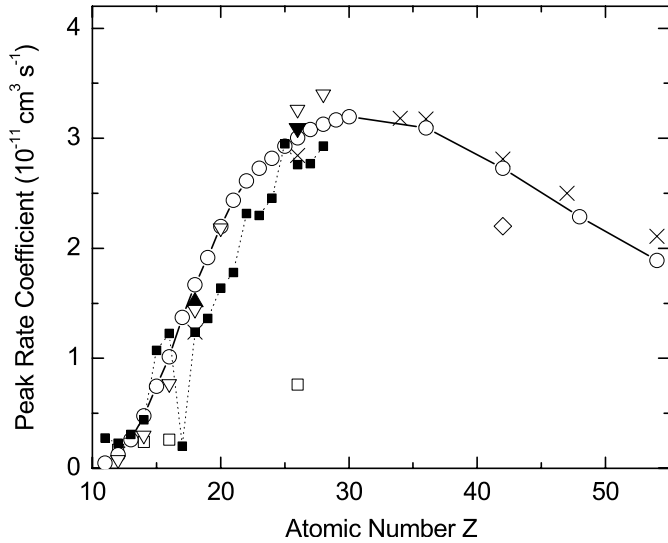
Fig. 5. Maximum total DR rate coefficients as a function of atomic number Z. The *open circles* represent our MCBP calculations. Comparison is given with the calculations of Jacobs et al. (1977, 1979, *open squares*), the Hartree-Fock distorted-wave calculation of Roszman (1979, *open diamond*), the MCDF calculations of Chen (1986, *crosses*), the compilation data of Mazzotta et al. (1998, *solid squares*), and with the relativistic DW calculations of Fournier et al. (1997, *solid up triangles*) and Gu (2003a, *solid down triangles*; 2003b, *open down triangles* . Lines are drawn through our data and those of Mazzotta et al. to guide the eye.

A simple way to compare various theoretical DR rate co-efficients along the entire neon-like isoelectronic series is to plot the maximum DR rate coefficient vs. the atomic number Z, as is done in Fig. 5. The results from the earlier calculations of Jacobs et al. (1977, 1979), as compiled by Shull & van Steenberg (1982), are obviously inaccurate. But more importantly, we also see considerable inaccuracies in the compiled data of Mazzotta et al. (1998). These data are based on the results of various calculations which used different methods and resorted to different approximations, and erratic behavior as a function of atomic number Z is clearly seen. For instance, the peak DR rate coefficient of Mazzotta et al. (1998) at $Z = 17$ is lower by almost an order of magnitude than the neighboring values at $Z = 16$ and $Z = 18$. Our results, which are in sufficient agreement with those of Chen (1986), show the expected smooth behavior with Z.

4. Summary

In this paper, we have systematically calculated partial and total DR rate coefficients along the neon-like sequence as part of an assembly of a DR database necessary for the modelling of finite-density plasmas (Badnell et al. 2003; Zatsarinny et al. 2003; Colgan et al. 2003). The approximations used for generating our data have been recently validated by the good agreement of DR resonance strengths and energies between our theoretical data and the experimental results for L-shell ions from the Test Storage Ring in Heidelberg. Comparisons have been made for systems such as lithium-like Si and Cu (Kilgus 1992), oxygen-like Fe (Savin et al. 2002), and fluorine-like Fe and Se

(Lampert et al. 1996; Savin et al. 1999), Since DR via $\Delta n = 1$ core excitations of these L-shell ions resembles DR of neon-like ions, we believe that a similar degree of accuracy was achieved in our present study as in past studies. Hence, for the accuracy of our results, we expect an $\approx 10\%$ variation when using different target orbitals, an $\approx 20\%$ difference when comparing to other state-of-the-art theory and an $\approx 30\%$ difference when comparing with laboratory measurements of $\Delta n = 1$ DR.

We have presented selected total DR rate coefficients for some ions of interest, and have made comparisons, where possible, with previous work. We found large discrepancies with previous calculations, including the fits of Mazzotta et al. (1998), which were used in their study of the ionization equilibrium for various atoms. Final-state-resolved rate coefficients have been tabulated, and these data are available from the web site http://www-cfadc.phy.ornl.gov/data_and_codes. Total DR and RR rate coefficients have been fitted by simple analytical formula which will prove of great use to astrophysical and fusion plasma modelers, and are available on our web site http://homepages.wmich.edu/~gorczyca/drdata.

We have calculated our data over a wide temperature range and for a large number of atomic ions in order to maximize the available information for plasma spectral modelling work. Our fits are accurate to better than 1% for all ions in the wide temperature range from 10^1 to 10^8 K. Because there are no $\Delta n = 0$ DR resonances for neon-like ions, the small uncertainties in the $\Delta n = 1$ DR resonance energies (whose energies are significantly larger than these uncertainties), have essentially no impact on our calculated rate coefficient. These RR and DR data are suitable for modelling of solar and cosmic plasmas under conditions of collisional ionization equilibrium, photoionization equilibrium, and non-equilibrium ionization (e.g., in shocks). Future papers will present DR data for further isoelectronic sequences as detailed previously (Badnell et al. 2003).

References

Arnaud, M., & Raymond, J. 1992, ApJ, 398, 396
Badnell, N. R. 1986, J. Phys. B, 19, 3827
Badnell, N. R. 1997, J. Phys. B, 30, 1
Badnell, N. R., & Pindzola, M. S. 1989, Phys. Rev. A, 39, 1690
Badnell, N. R., O'Mullane, M., Summers, H. P., et al. 2003, A&A, 406, 1151
Berrington, K. A., Eissner, W. B., & Norrington, P. H. 1995, Comput. Phys. Commun., 92, 290
Chen, M. H. 1986, Phys. Rev. A, 34, 1073
Colgan, J., Pindzola, M. S., Whiteford, A. D., & Badnell, N. R. 2003, A&A, 412, 597
Froese Fisher, C. 1991, Comput. Phys. Commun., 64, 369
Fournier, K. B., Cohen, M., & Goldstein, W. H. 1997, Phys. Rev. A, 56, 4715

Gorczyca, T. W., Badnell, N. R., & Savin, D. W. 2002, Phys. Rev. A, 65, 062707

Gu, M. F. 2003a, ApJ, 582, 1241

Gu, M. F. 2003b, ApJ, 590, 1131

Jacobs, V. L., Davis. J., Kepple, P. C., & Bhala, M. 1977, ApJ, 211, 605; 215, 690

Jacobs, V. L., Davis, J., Rogerson, J. E., & Bhala, M. 1979, ApJ, 230, 627

Kilgus, G., Habs, D., Schwalm, D., et al. 1992, Phys. Rev. A, 46, 5730

Lampert, A., Wolf, A., Habs, D., et al. 1996, Phys. Rev. A, 53, 1413

Landini, M., & Monsignori Fossi, B. C. 1991, A&AS, 91, 183L

Mazzotta, P., Mazzitelli, G., Colafrancesco, S., & Vittorio, N. 1998, A&AS, 133, 403

Ramirez, J. M., & Bautista, M. 2002, J. Phys. B, 35, 4139

Romanik, C. J. 1988, ApJ, 330, 1022

Roszman, L. J. 1979, Phys. Rev. A, 20, 673

Savin, D. W., Kahn, S. M., Linkemann, J., et al. 1999, ApJS, 123, 687

Savin, D. W., & Laming, J. M. 2002, ApJ, 566, 1166

Savin, D. W., Kahn, S. M., Linkemann, J., et al. 2002, ApJ, 576, 1098

Shull, J. M., & van Steenberg, M. 1982, ApJS, 46, 95

Summers, H. P. 1999, ADAS User Manual (2nd Edition), available from `http://adas.phys.strath.ac.uk/adas/docs/manual`

Verner, D. A., & Ferland, G. J. 1996, ApJS, 103, 467

Zatsarinny, O., Gorczyca, T. W., Korista, K., Badnell, N. R., & Savin, D. W. 2003, A&A, 412, 587